



OPEN

Protective capacity of carotenoid trans-astaxanthin in rotenone-induced toxicity in *Drosophila melanogaster*

Temitope C. Akinade¹, Oreoluwa O. Babatunde¹, Adeola O. Adedara¹, Olugbenga E. Adeyemi², Titilayomi A. Otenaike¹, Onaara P. Ashaolu³, Titilayo O. Johnson², Ana Terriente-Felix⁴, Alexander J. Whitworth⁴✉ & Amos O. Abolaji¹✉

Trans-astaxanthin (TA), a keto-carotenoid found in aquatic invertebrates, possesses anti-oxidative and anti-inflammatory activities. Rotenone is used to induce oxidative stress-mediated Parkinson's disease (PD) in animals. We probed if TA would protect against rotenone-induced toxicity in *Drosophila melanogaster*. Trans-astaxanthin (0, 0.1, 0.5, 1.0, 2.5, 10, and 20 mg/10 g diet) and rotenone (0, 250 and 500 μ M) were separately orally exposed to flies in the diet to evaluate longevity and survival rates, respectively. Consequently, we evaluated the ameliorative actions of TA (1.0 mg/10 g diet) on rotenone (500 μ M)-induced toxicity in *Drosophila* after 7 days' exposure. Additionally, we performed molecular docking of TA against selected pro-inflammatory protein targets. We observed that TA (0.5 and 1.0 mg/10 g diet) increased the lifespan of *D. melanogaster* by 36.36%. Moreover, TA (1.0 mg/10 g diet) ameliorated rotenone-mediated inhibition of Catalase, Glutathione-S-transferase and Acetylcholinesterase activities, and depletion of Total Thiols and Non-Protein Thiols contents. Trans-astaxanthin prevented behavioural dysfunction and accumulation of Hydrogen Peroxide, Malondialdehyde, Protein Carbonyls and Nitric Oxide in *D. melanogaster* ($p < 0.05$). Trans-astaxanthin showed higher docking scores against the pro-inflammatory protein targets evaluated than the standard inhibitors. Conclusively, the structural features of TA might have contributed to its protective actions against rotenone-induced toxicity.

Exposure to rotenone has been implicated in the pathophysiology of Parkinson's disease (PD) in both animals and humans via mechanisms associated with oxidative stress and mitochondrial dysfunction. Indeed, exposure to rotenone extends beyond occupational setting as inadvertent non occupational exposures to rotenone via pesticides in the environment has been reported¹. Rotenone is a member of rotenoids, that consists of a central dihydro- γ -pyrone ring which is proposed to be responsible for rotenone-mediated mitochondrial toxicity². Rotenone is metabolized by CYP 3A4 or 2C19 to hydroxyl rotenone in the liver of rats and the mid-gut of insects³. Rotenone strongly inhibits mitochondrial complex I, blocks electron transport chain, increase electron leakage and produces energy deficit⁴. This results in excessive production of mitochondrial-ROS, which overcomes the capacity of the antioxidants system such as superoxide dismutase, catalase and glutathione peroxidase⁵. This then elicits oxidative damage to macromolecules and apoptosis of non-neuronal and neuronal cells^{6,7}. The capacity of rotenone to penetrate Blood Brain Barrier (BBB) enables neuronal assault⁷. Additionally, rotenone inhibits microtubule assembly leading to mitotic arrest⁷. It also elicits the formation of cytosolic Lewy bodies and microglial activation in animals⁸.

Accumulation of Reactive Oxygen and Nitrogen Species (RONS) due to exposure to toxicants, can cause oxidative damage to biomolecular constituents of the cells and organelles^{6,9}. Thus, search is ongoing for natural

¹Drosophila Laboratory, Department of Biochemistry, Molecular Drug Metabolism and Toxicology Unit, Faculty of Basic Medical Sciences, College of Medicine, University of Ibadan, Ibadan, Nigeria. ²Department of Biochemistry, Faculty of Basic Medical Sciences, College of Health Sciences, University of Jos, Jos, Nigeria. ³Department of Physiology, Faculty of Basic Medical Sciences, College of Medicine, University of Ibadan, Ibadan, Nigeria. ⁴MRC Mitochondrial Biology Unit, University of Cambridge, Cambridge, UK. ✉email: a.whitworth@mrc-mbu.cam.ac.uk; ao.abolaji@ui.edu.ng

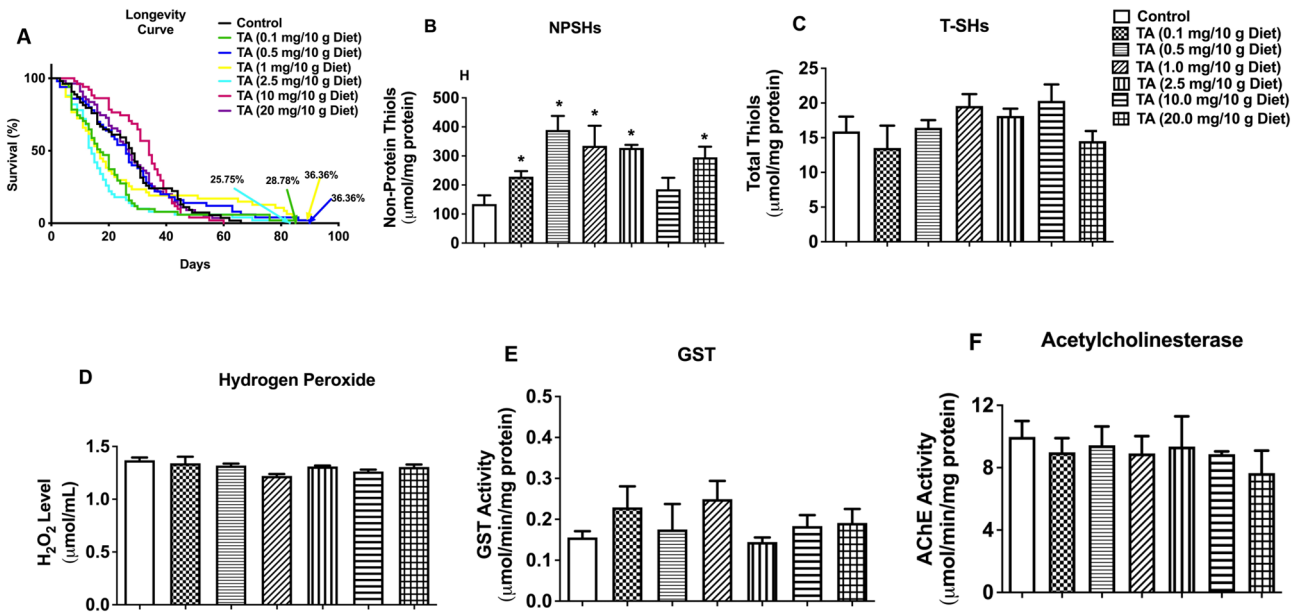


Figure 1. Effects of TA (0.1, 0.5, 1.0, 2.5, 10, and 20 mg/ 10 g diet) on longevity (A), levels of NPSHs (B), T-SHs (C) and H_2O_2 (D), and activities of the enzymes GST (E) and AChE (F) in *D. melanogaster*. Data in (B–F) are presented as mean \pm SEM of 50 flies per vial (five replicates per group). *Significant difference compared with control group ($p < 0.05$). TA trans-astaxanthin, NPSHs non-protein thiols, T-SHs total thiols, GST glutathione-S-transferase, AChE acetylcholinesterase.

products with antioxidative and anti-inflammatory activities that can be used to prevent or reduce oxidative damage-induced diseases elicited by exposure to environmental contaminants.

Trans-astaxanthin (TA) is a natural red pigment (lipid-soluble keto-carotenoid member of xanthophylls) and precursor of vitamin A^{10,11}. It can be commercially derived from lower plants (microalgae: *Haematococcus pluvialis*), aquatic animals (crustaceans and salmon etc.) or chemically synthesized¹². It is also known as all-trans-astaxanthin, astaxanthin, E-astaxanthin, (S,S)-astaxanthin, astaxanthin or 3,3'-dihydroxy- β , β' -carotene-4,4'-dione¹³. It can exist as geometric- (cis or trans) or stereo- (Sinister or Rectus) isomers. The trans- and S-isomers are more stable than the Cis-isomer with higher bioactivity¹⁴. TA possesses much higher bioactivity than other carotenoids owing to its inherent polar ends [hydroxy (OH) and keto (C=O) on both terminal ends and nonpolar central moiety (polyene system or conjugated carbon-carbon double bonds (–C=C–C=C–)] in its chemical structure^{12,15}. Therefore, the polyene system allows it to intercalate and also cross the BBB¹⁶. Both the polar and nonpolar moieties play significant roles in preventing the cells from oxidative damage by scavenging radicals, quenching singlet oxygen, inhibiting lipid peroxidation and regulating oxidative stress-mediated gene expression^{17,18}. Furthermore, TA can form complexes with both lipoproteins and proteins to form carotenolipoproteins and carotenoproteins, respectively. It can diffuse through the BBB, thereby protecting the brain from acute injury and chronic neurodegeneration¹⁹. Interestingly, evidences of anti-inflammatory, immunomodulatory, antioxidant²⁰ and neuroprotective activities²¹ of TA are available in the literature.

Drosophila melanogaster has been utilized as a model for testing the protective efficacy of natural compounds in the context of neurodegenerative diseases, including Parkinson's disease model using rotenone-exposed or transgenic *Drosophila melanogaster*²². *Drosophila* has low or absent ethical limitations, short life cycle, high fecundity and low cost of maintenance^{9,23,24}. In addition, it is being used to model human disease phenotypes, such as PD^{22,25}. Chronic administration of rotenone to flies has been shown to cause selective degeneration of dopaminergic neurons, neuroinflammation and locomotor abnormality^{26,27}. The use of TA to treat and attenuate the debilitating effects of rotenone-induced toxicity has not been reported. Therefore, in this study, we aimed to investigate the protective capacity of TA in rotenone-induced toxicity in flies as well as its molecular targets through molecular docking analyses.

Results

Effects of exposure to graded doses of TA on longevity, oxidative stress status and acetylcholinesterase activity in *D. melanogaster*. The TA concentrations of 0.5 and 1.0 mg/10 g diet both increased longevity by 36.36% compared to the control (Fig. 1A). Seven days of exposure of flies to TA indicated no adverse effects on NPSHs (Fig. 1B), T-SHs (Fig. 1C), H_2O_2 (Fig. 1D), GST (Fig. 1E) and AChE (Fig. 1F). In addition, TA significantly boost the level of NPSHs compared with the control ($p < 0.05$). Considering the fact that 0.5 and 1.0 mg/10 g diet concentrations of TA induced the highest effect on the lifespan of flies than the other concentrations, we selected 1.0 mg/10 g of diet concentration to investigate its protective role in rotenone-induced toxicity in *Drosophila melanogaster*.

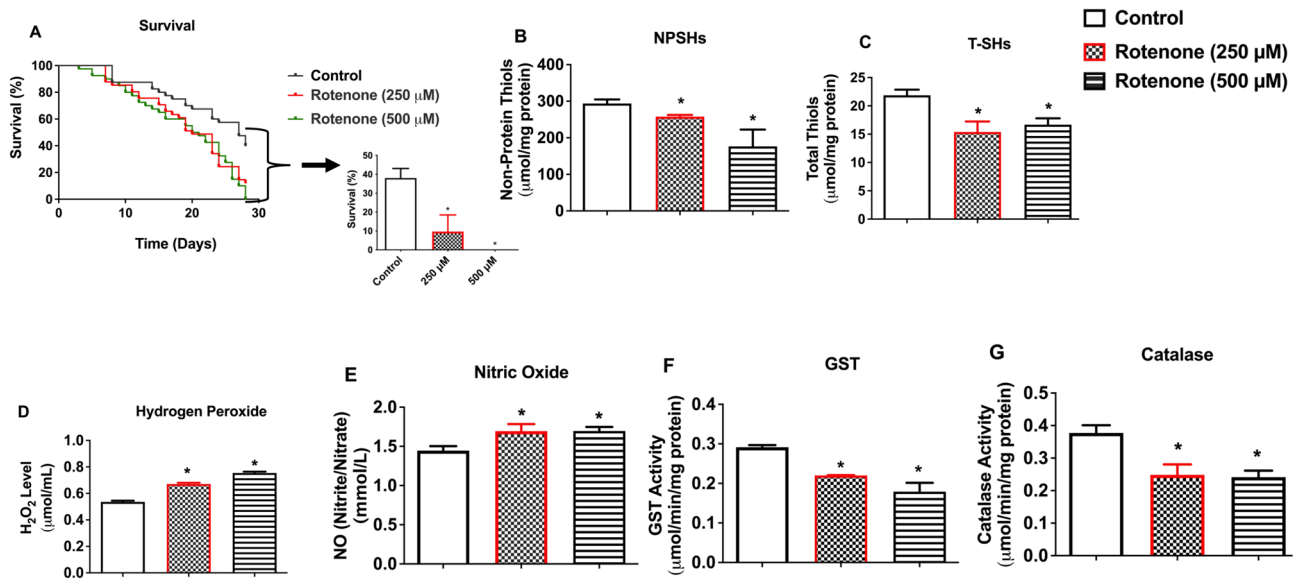


Figure 2. Effects of rotenone (250 and 500 μM) on 30-day survival rate (A), levels of NPSHs (B), T-SHs (C), H_2O_2 (D), NO (E), and activities of the enzymes GST (F) and Catalase (G) in *D. melanogaster*. Data in (A–G) are presented as Mean \pm SEM of 50 flies per vial (five replicates per group). *Significant difference compared with control group ($p < 0.05$). NPSHs non-protein thiols, T-SHs total thiols, H_2O_2 hydrogen peroxide, GST glutathione-S-transferase, AChE acetylcholinesterase

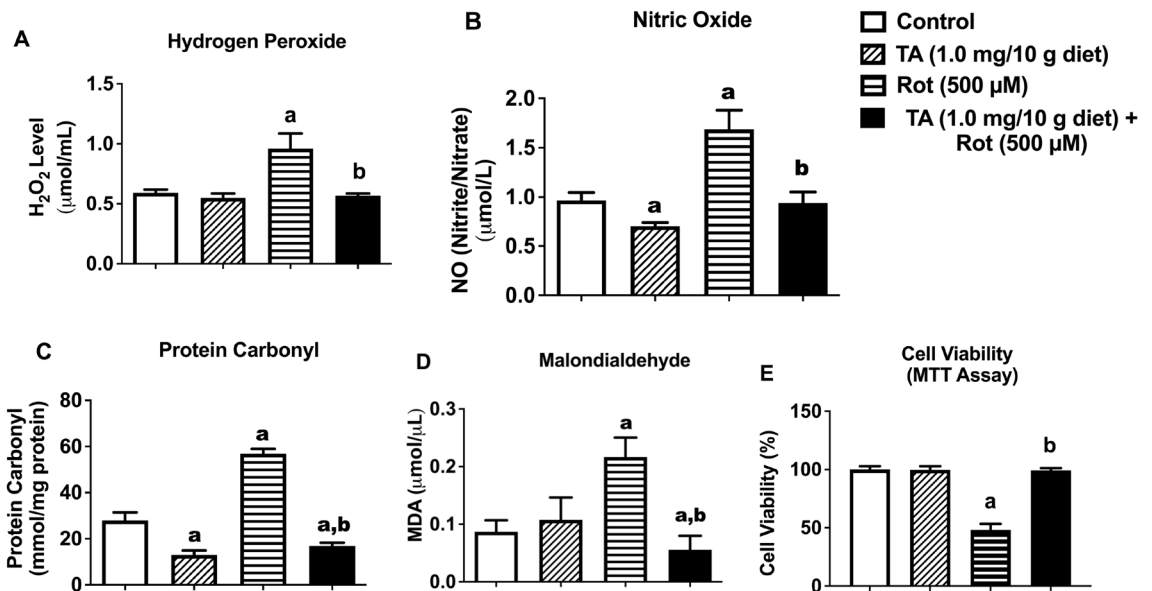


Figure 3. Effects of TA (1.0 mg/10 g diet) and/or rotenone (500 μM) on H_2O_2 (A), NO (B), Protein Carbonyl (C), Malondialdehyde (D), and Cell Viability (MTT assay) (E). Data in (A–E) are presented as Mean \pm SEM of 50 flies per vial (five replicates per group). a: Significant difference compared with control group; b: Significant difference compared with rotenone group ($p < 0.05$). TA trans-astaxanthin, H_2O_2 hydrogen peroxide.

Rotenone exposure impairs survival rate and alters antioxidative status and inflammatory marker in *D. melanogaster*. Rotenone significantly reduced survival rate of *D. melanogaster* after 30 days of treatment compared with the control (Fig. 2A, $p < 0.05$). Additionally, rotenone significantly reduced NPSHs (Fig. 2B) and T-SHs (Fig. 2C) and elevated H_2O_2 (Fig. 2D) and NO (Fig. 2E) levels compared with the control. Apart from this, rotenone inhibited activities of GST (Fig. 2F) and Catalase (Fig. 2G) compared with the control flies ($p < 0.05$). Consequently, 500 μM dose of rotenone was selected in the ameliorative study with TA.

TA attenuates rotenone-induced increased levels of oxidative stress and inflammatory markers, and reduced cell viability in *D. melanogaster*. TA restored to normal, rotenone-induced elevation of H_2O_2 (Fig. 3A), nitric oxide (Fig. 3B, nitrite/nitrate), and blocked the increase of protein carbonyl (Fig. 3C),

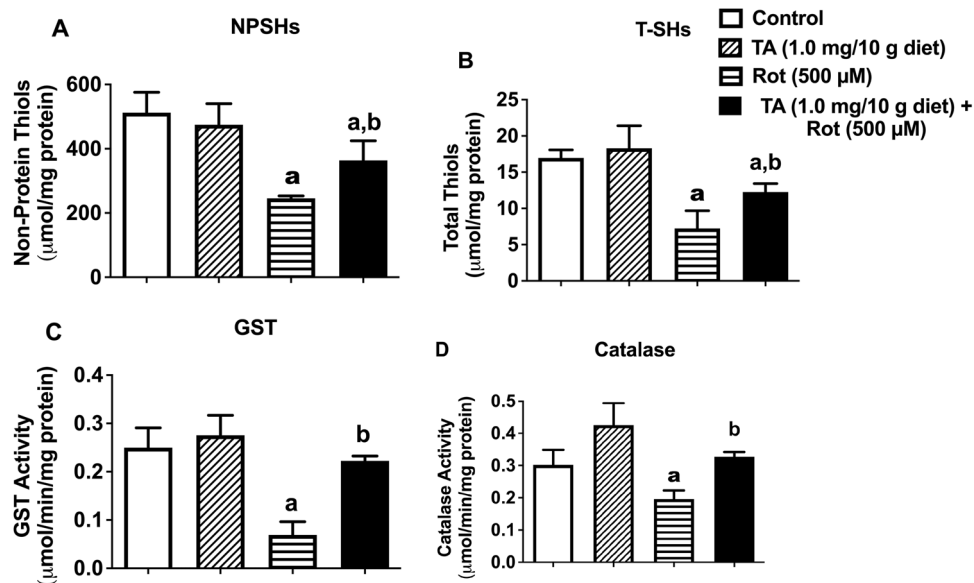


Figure 4. Effects of TA (1.0 mg/10 g diet) and/or rotenone (500 μM) on Levels of NPSHs (A), T-SHs (B), and activities of the enzymes GST (C) and Catalase (D). Data in (A–D) are presented as Mean ± SEM of 50 flies per vial (five replicates per group). a: Significant difference compared with control group; b: Significant difference compared with rotenone group ($p < 0.05$). TA trans-astaxanthin, NPSHs non-protein thiols, T-SHs total thiols, GST glutathione-S-transferase.

and malondialdehyde (Fig. 3D, $p < 0.05$). In addition, TA attenuated rotenone-induced reduction in mitochondrial metabolic rate (cell viability) assessed by MTT assay in *D. melanogaster* (Fig. 3E).

TA Restores the antioxidant status impaired by rotenone in *D. melanogaster*. The effects of rotenone and TA on NPSHs, T-SHs, catalase and GST are shown in Fig. 4. Indeed, TA partially prevented rotenone-induced depletion of NPSHs (Fig. 4A) and T-SHs (Fig. 4B) contents and ameliorated rotenone-induced inhibition of GST (Fig. 4C) and catalase (Fig. 4D) activities in *D. melanogaster*.

TA improved behavioral dysfunction and acetylcholinesterase activity and did not alter reduced emergence rate induced by rotenone in *D. melanogaster*. The effects of rotenone and TA on negative geotaxis (locomotor activity), emergence rate and AChE are shown in Fig. 5. We found that although TA ameliorated rotenone-induced behavioural deficit (Fig. 5A, $p < 0.05$), it could not rescue rotenone-induced reduction of emergence rate of progeny of flies (Fig. 5B, $p > 0.05$). In addition, TA partially attenuated rotenone-induced inhibition of AChE activity (Fig. 5C).

Molecular docking analysis. The docking scores of TA was higher than those of the standard inhibitors (Rofecoxib, Pralnacasan and Thalidomide) for the inflammatory protein targets (TNF- α , Caspase-1 and Cox-2) in both *D. melanogaster* and *H. sapiens*, except for *Drosophila* caspase-1 (DmCasp-1) where the docking score of Pralnacasan (−7.8 kcal/mol) was lower compared with that of TA which was −7.2 kcal/mol (Table 1).

Also, TA occupied the binding pockets of the respective standard inhibitors for all the protein targets, thus, sharing similar amino acids for interactions at the active sites (Fig. 6).

TA and Thalidomide interacted with the triad amino acid residues (His 281, Ala 279 and Arg 277) of the active site of the DmTNF- α . Both compounds also interacted with common amino acid residues at the active pocket of HsTNF- α (Fig. 6A–D). Both TA and Rofecoxib bound to Val 291 and Lys 211 residues of the active pocket of HsCox-2, and to Tyr 193, Phe 192 and Phe 133 triad residues of the *Drosophila* homolog of the same enzyme (Fig. 7E–H). The interactions of the natural compound and the caspase-1 inhibitor (pralnacasan) at the binding pockets of the human protein target (HsCasp-1) occurred with Ile 155, Trp 145 and Ala 141 residues; and of the *Drosophila* homologue (DmCasp-1) with Thr 308 residue (Fig. 8I–L). Nonetheless, TA seemed to form strong hydrogen bonds, in addition to several other bond types (alkyl and van der Waal forces) (Figs. 6A–D, 7E–H, 8I, J).

Discussion

Rotenone has been established to induce neurodegenerative diseases such as PD in animals including *Drosophila melanogaster*. Some of the hallmark features of PD include oxidative stress, inhibition of mitochondrial complex I, dopaminergic neuronal loss and locomotor abnormality^{4,26,27}. However, the use of trans-astaxanthin (TA) to treat and attenuate the debilitating effects rotenone-induced toxicity in *D. melanogaster* is scarce in the literature. Here, we investigated the protective capacity of TA on rotenone-induced toxicity using *D. melanogaster* as

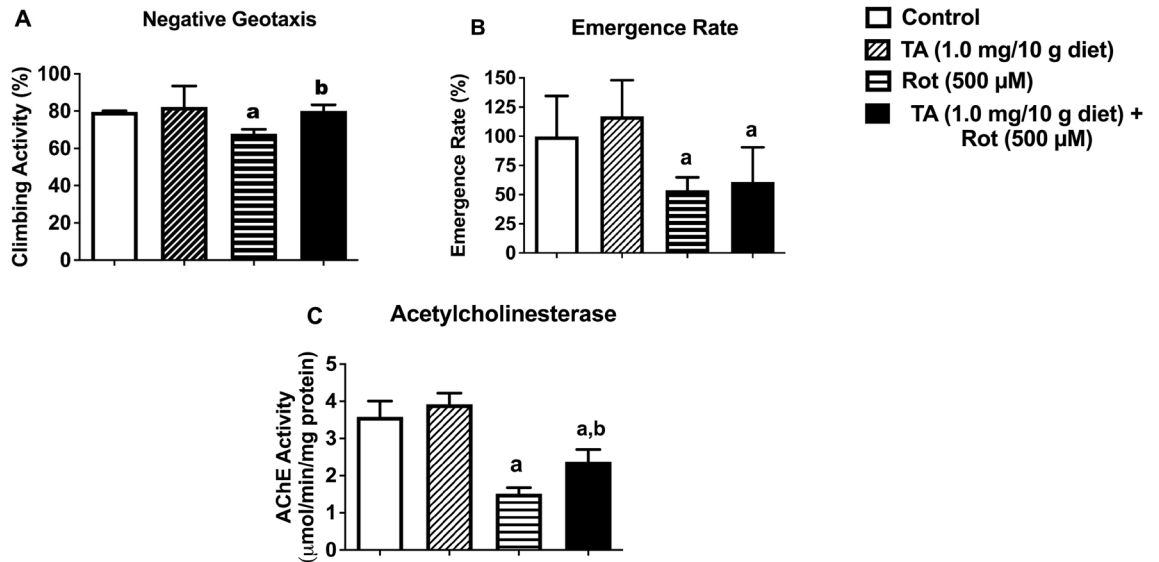


Figure 5. Effects of TA (1.0 mg/10 g diet) and/or rotenone (500 µM) on emergence rate (A), and acetylcholinesterase activity (B). Data in (A–C) are presented as Mean ± SEM of 50 flies per vial (five replicates per group). a: Significant difference compared with control group; b: Significant difference compared with rotenone group (p < 0.05). TA trans-astaxanthin.

Standard nhibitors	PubChem CID	ΔG energy (Kcal/mol)					
		DmTNF-α	HsTNF-α	DmCasp-1	HsCasp-1	DmCox-2	HsCox-2
TA	5281224	-6.8	-7.7	-7.2	-8.3	-7.6	-7.3
Pralnacasan	153270			-7.8	-8.1		
Rofecoxib	5426	-6.0	-6.5				
Thalidomide	5090					-5.8	-6.6

Table 1. Binding affinities of trans-astaxanthin (TA) and some standard inhibitors for the selected anti-inflammatory protein targets. Dm: *Drosophila melanogaster*; hm: human, TNF-α: tumour necrosis factor-alpha (Eiger in *Drosophila*), Caspase-1 (Dcp-1 (*Drosophila* caspase-1) in *Drosophila*); and Cox-2 (COII (cytochrome oxidase subunit 2) in *D. melanogaster*).

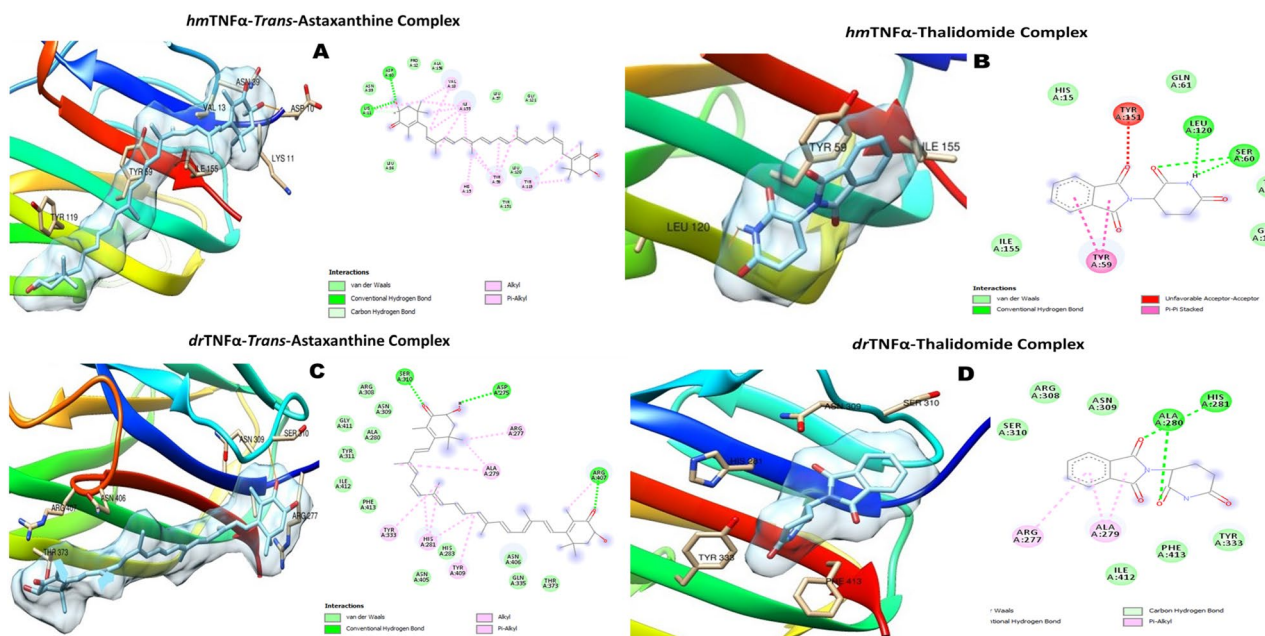


Figure 6. The 3D and 2D molecular complexations of Human TNFα (hmTNFα) with TA (A) and Thalidomide (B), and Drosophila TNFα (drTNFα) with TA (C) and Thalidomide (D) respectively.

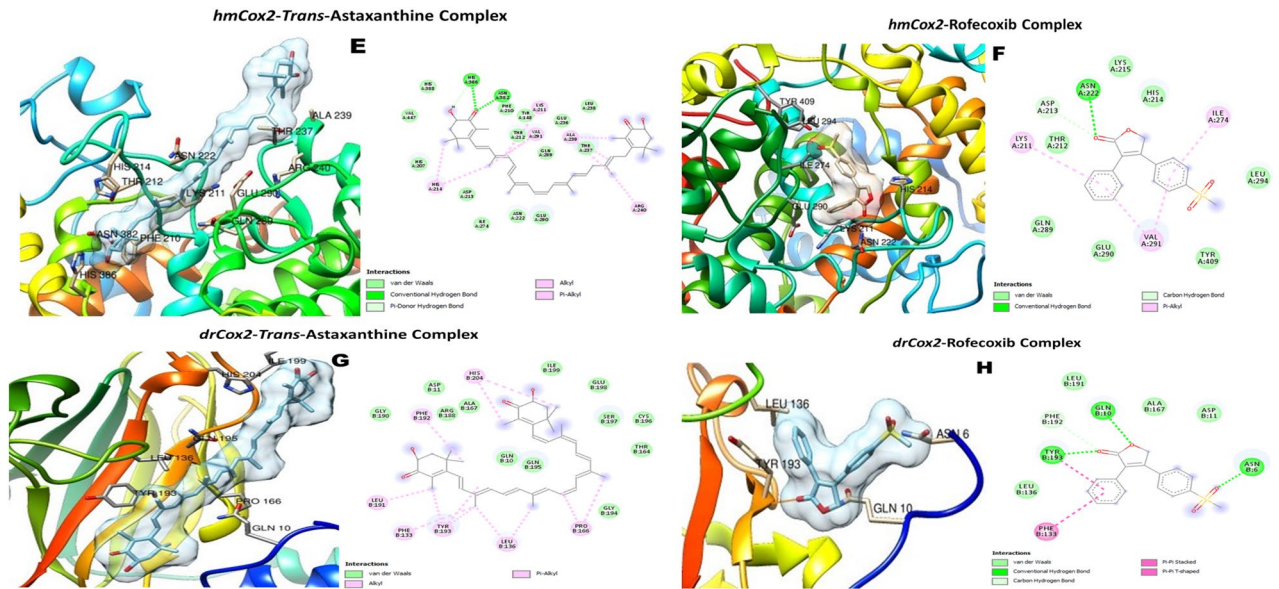


Figure 7. The 3D and 2D molecular complexations of Human Cox2 (hmCox2) with TA (E) and Rofecoxib (F); and *Drosophila* Cox-2 (drCox-2) with TA (G) and Rofecoxib (H) respectively.

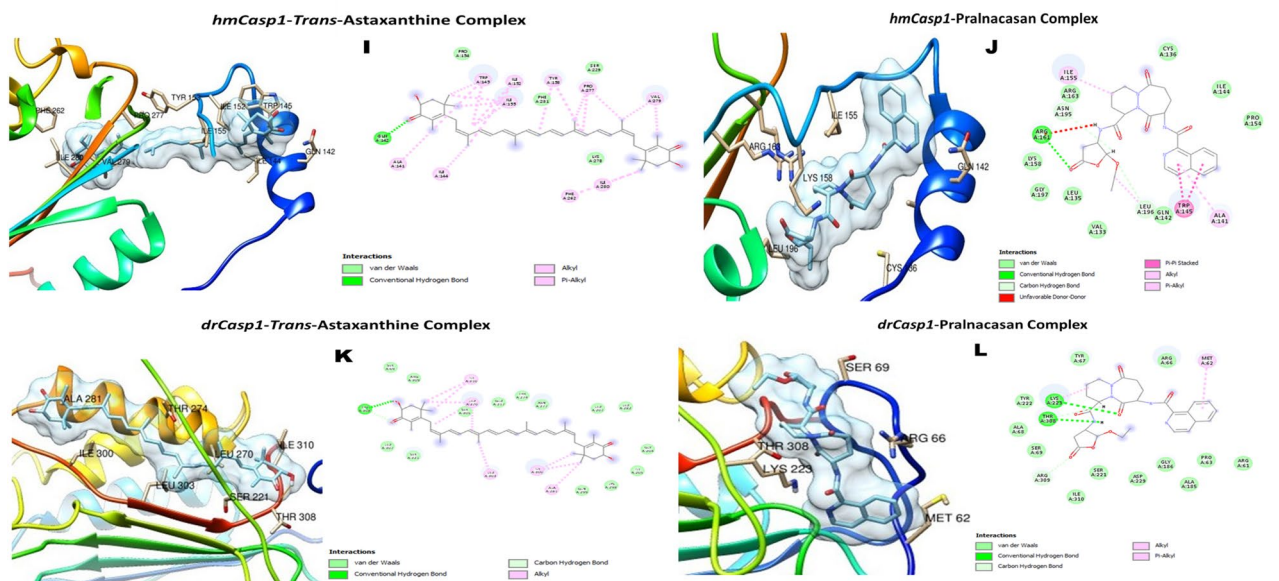


Figure 8. The 3D and 2D molecular complexations of Human Caspase-1 (hmCasp-1) with TA (I) and Pralnacasan (J); and *Drosophila* Caspase-1 (drCasp-1) with TA (K) and Pralnacasan (L) respectively.

a model. We evaluated different behavioural and oxidative stress markers as well as molecular mechanisms of actions of TA against inflammatory protein targets using in silico approach.

From the different concentrations of TA used in this study, 0.1, 0.5, 1.0 and 2.5 mg/10 g diet prolonged the lifespan of flies by 28.78, 36.36, 36.36 and 25.75%, respectively, compared with the control. This suggests that TA might possess anti-aging activity by extending the lifespans of the flies. Our finding is in support of the report of Huangfu et al.²⁸ showing that TA has pro-longevity activity against *SOD1* null mutant flies by protecting against oxidative stress. It also corroborates the lifespan extension in *C. elegans* by preventing against oxidative stress through interaction with mitochondrial complex III electron leakage²⁹.

Acetylcholine (ACh) and Dopamine (DA) are the major antagonistic neurotransmitters, released from the striatal cholinergic interneurons (SCI) and substantia nigra (SNi) neurons, respectively, onto the dorsal striatum of the midbrain³⁰. Membrane-bound post-synaptic acetylcholinesterase (AChE) liberates choline and acetyl group from ACh into the synaptic cleft, thereby alleviating cholinergic toxicity that is responsible for the motor symptoms, such as bradykinesia, tremor and rigidity, observed in PD³¹. Several studies have indicated an altered

AChE activity by rotenone in different animal models, including *D. melanogaster*^{4,32}. In this study, we found that the inhibition of AChE activity by rotenone in *D. melanogaster*, was coupled with impaired locomotor activity. Interestingly, we found that TA improved the rotenone-induced inhibition of AChE activity and decline in locomotor performance of the flies.

The observed rotenone-induced accumulation of H₂O₂ and inhibition of catalase activity are indications of oxidative damage. Indeed, rotenone has been shown to inhibit mitochondrial complex I leading to electron leakage and superoxide radical production that in turn dismutated to H₂O₂ by superoxide dismutase. The elevated H₂O₂ can produce reactive and short-lived hydroxyl radical (OH·) through Fenton reaction, which in turn can induce oxidative damage to proteins, nucleic acids and lipid components⁵. These observations prompted us to corroborate the fact that, indeed, TA possesses antioxidative property against ROS^{17,18}.

The observed inhibition of Glutathione-S-transferases (GST) in the rotenone-exposed flies might suggest GST's dysfunctional detoxification capacity^{9,33}. The observation that TA ameliorated rotenone-induced inhibition of GST further strengthens its antioxidative capacity. Consequently, we evaluated thiols' status of the *D. melanogaster*. Thiols are carbon-bound sulfhydryls (SHs) chemical groups. They are classified into protein thiols and non-protein thiols (NPSHs), in which the latter is majorly composed of GSH, besides other thiols³⁴. The thiols are involved in many physiological roles among which is tissue protection against oxidative damage²⁸. Low level of thiols has been associated with many cellular dysfunctions, aging and neurodegenerative diseases, including PD^{35,36}. Hence, decreased level of NPSHs has been reported in both PD patients and experimental models of PD³⁷, including rotenone-induced PD model in flies³⁸. In this study, TA restored the protective status of both total thiols and NPSHs, that were depleted in flies treated with rotenone.

We further evaluated other oxidative stress markers such as protein carbonyls (PCs) and malondialdehyde (MDA, a product of lipid peroxidation). In fact, different products of PCs are generated from oxidative assault to amino acid side chains or backbone cleavage in a protein by hydroxyl radicals³⁹. PCs formed by the product of lipid peroxidation, such as MDA, has been used to accentuate the oxidative source of PCs⁴⁰. Aging tissues and neurodegenerative diseases have been shown to be associated with increased levels of PCs and lipid peroxidation product⁴⁰. Studies have reported elevated levels of PCs and MDA in *D. melanogaster* fed with rotenone⁴⁰. Interestingly, we found that inclusion of TA in the diet reversed rotenone-induced elevation of PCs and MDA in flies.

Also, we sought to understand whether toxicity induced by rotenone reduced cell viability by carrying out MTT assay, which is a measure of cellular and mitochondrial metabolic rate. We found that rotenone indeed reduced cell viability in the flies. Strikingly, TA ameliorated rotenone-induced reduction of cell viability in *D. melanogaster*. Moreover, we carried out emergence rate of progenies of flies and found that TA did not attenuate rotenone-induced reduction in emergence rate.

Nitric oxide [NO, (nitrite/nitrates)] can react with superoxide anion radical to form a more poisonous oxidative species (ONOO·, peroxynitrite) that have been evidenced in many pathologies⁴¹. This pro-inflammatory marker is physiologically released during inflammatory burst by the immune cells. However, in diseased state, NO is uncontrollably released in an accumulative manner. This, consequently, can lead to the production of peroxynitrite and other pro-inflammatory markers that results in cellular apoptosis⁴². The remarkable amelioration of rotenone-mediated elevation of NO by TA confirms that it possesses anti-inflammatory activity.

Molecular docking analysis was performed to provide further insight into the molecular mechanism of the anti-inflammatory capacity of TA against rotenone-induced inflammation. Tumour necrosis factor-alpha (TNF- α), Cyclooxygenase-2 (Cox-2) and Caspase-1 (Casp-1) are the pro-inflammatory mediators accompanied with NO release, through NF- κ B and inflammasome complex-mediated responses^{43,44}. These proteins are members of the group of pro-inflammatory markers that might be stimulated or released by glial cells, as a result of the signalling interplays of their molecular origins, during chronic neuroinflammation-induced PD⁴⁵⁻⁴⁷. The Cox-2, TNF- α , and Caspase-1 have been implicated in the neuroinflammation-mediated PD⁴⁸. The inhibition of these three protein targets are windows of opportunity for a new anti-PD drug development. In the light of this, TA was subjected to molecular docking against human TNF- α , Cox-2 and Casp-1 protein targets, as well as their *Drosophila* homologues. Interestingly, TA showed higher docking scores against both the human and *Drosophila* proteins than the standard inhibitors except for the Pralnacasan against DmCasp-1. The molecular interactions of TA with the anti-inflammatory protein targets could be the mechanisms employed by TA to regulate the inflammatory response triggered by exposure of flies to rotenone. The increased binding affinity of TA to target proteins can be attributed to different factors, such as the more negative change in free energy, the interaction of its different functional groups with the amino acid residues at the active pockets of the proteins, and the nature of the binding that occurred between them^{49,50}. These molecular interactions depend on the chemical structure of TA which contains the keto- (C=O) and hydroxyl (OH-) groups on the two terminal β -ionone rings and the central conjugated carbon (-C=C-C=C-) group joining the two β -ionone rings. The C=O and OH- groups on the β -ionone ring formed different types of hydrogen bonds (conventional, carbon-hydrogen and pi-donor), being the strongest noncovalent bond, with the amino acids at the active sites of the human and *Drosophila* protein targets. Additionally, the polyene group, as well as free carbon-hydrogen (C-H) was also responsible for hydrophobic bond types such as alkyl and pi-alkyl. Likewise, van der Waal forces do exist. Thus, TA, using its hydroxyl group, was strongly hydrogen-bonded with Asp10 and Lys11 at the binding site of the human TNF- α , and also with Asp275, and Ser310 and Arg407, using hydroxyl and keto groups, respectively, at the binding site of the *Drosophila* homologue of TNF- α . Also, His386 and Asn382 at the binding pocket of human Cox-2 were tightly hydrogen bonded with both hydroxyl and carbonyl oxygen of the β -ionone ring of the TA, whereas it was the carbon-hydrogen of the ring and the conjugated bonds in the bioactive compound that formed several alkyl bonds with many amino acids at the active site of Cox-2 homologue of *D. melanogaster*. Nonetheless, many alkyl bonds and van der Waal forces of the carbon-hydrogen and polyene bonds in the TA with several amino acids in the binding site of the human Caspase-1 could also be responsible for the higher binding affinity.

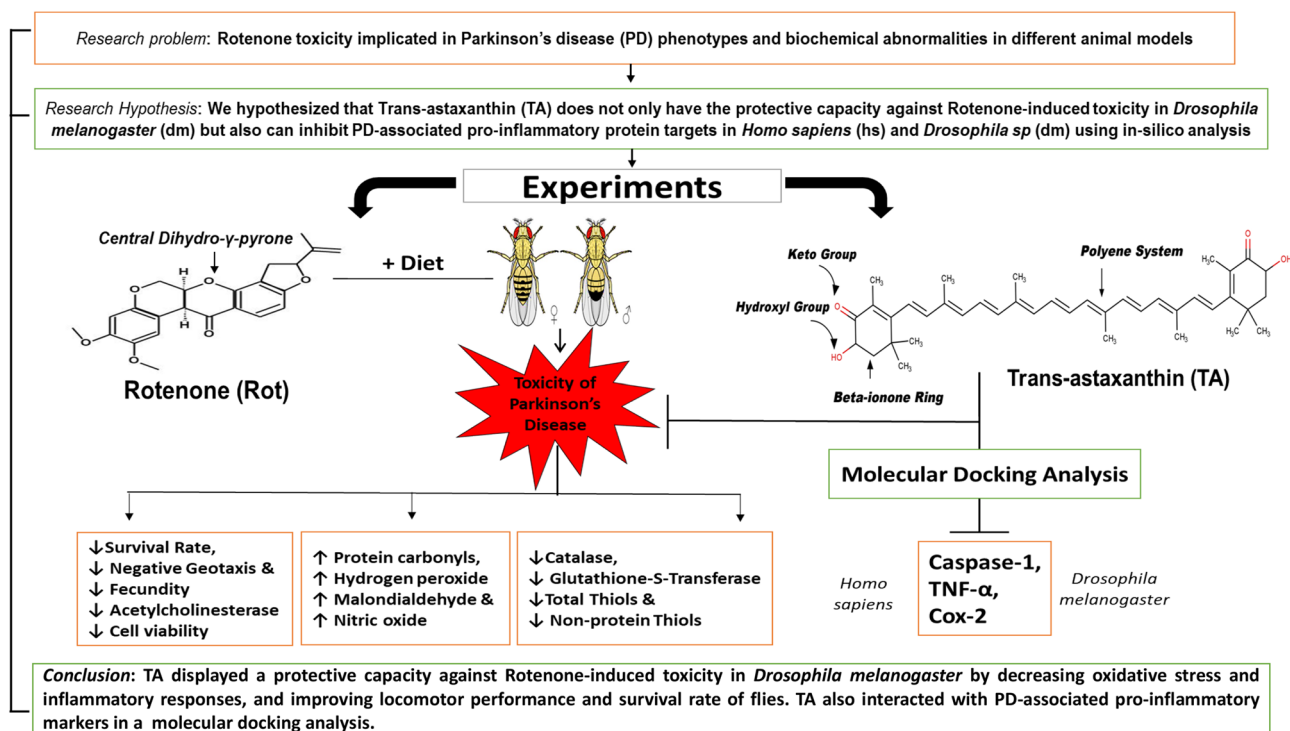


Figure 9. A flowchart showing an overview of experimental steps and outcome.

In conclusion, rotenone-induced toxicity is due to the perturbation of redox system, leading to oxidative stress, inflammation and behavioural abnormalities in flies. Interestingly, TA exhibited protection against rotenone-induced oxidative damage by enhancing endogenous antioxidant capacity, decreasing oxidative stress markers, and inflammation. Moreover, the interaction of the central polyene system as well as carbonyl and hydroxyl functional moieties of the two terminal β -ionone rings of TA, contribute to its antioxidative and anti-inflammatory properties (Fig. 9). Thus, TA can be considered as a promising therapeutic compound against oxidative stress and inflammation induced by rotenone and or related pesticides and insecticides.

Materials and methods

Chemicals. All chemicals used were commercial products of analytical grade. Trans-astaxanthin (TA) and rotenone were procured from AK Scientific, 30023 Ahern Ave, Union City, CA 94587, USA.

***Drosophila melanogaster* stock and culture.** *D. melanogaster* wild-type (Harwich strain) flies, that were obtained from National Species Stock Center (Bowling Green, OH, USA), were maintained and reared in *Drosophila* Laboratory, Biochemistry Department, University of Ibadan, Nigeria on cornmeal medium containing 1% w/v brewer's yeast, 2% w/v sucrose, 1% w/v powdered milk, 1% w/v agar, and 0.08% v/w nipagin at constant temperature and humidity (22–24 °C; 60–70% relative humidity) under 12 h dark/light cycle conditions.

Treatment of *D. melanogaster* with TA and rotenone. In order to select suitable concentrations and duration of exposure of flies to TA and rotenone, we carried out longevity and 30-day survival assays, respectively. Based on the longevity and survival data obtained, 7 days was chosen as duration to evaluate individual effects of TA (0, 0.1, 0.5, 1.0, 2.5, 10, and 20 mg/10 g diet) and rotenone (0, 250 and 500 μ M/10 g diet) on some selected biochemical markers. Thereafter, the flies were anaesthetized on ice, weighed, homogenized in 0.1 M phosphate buffer (pH 7.4, ratio of 1 mg:10 μ L) and centrifuged at 4000 \times g for 10 min at 4 °C in a thermo scientific Sorval Legend Micro 7R centrifuge. Supernatants were collected, stored at –20 °C and used for the determination of the following biochemical parameters: Non-Protein Thiol (NPSHs), Total Thiol (T-SHs), Hydrogen peroxide (H₂O₂), Nitric Oxide (NO, nitrate and nitrite), catalase, Glutathione-S transferase (GST), and Acetylcholinesterase (AChE)³³.

From the data obtained above, we selected 1.0 mg/10 g diet of TA to understand its protective capacity on rotenone (500 μ M)-induced toxicity after 7 days of treatment as follows:

- Group 1 (Control, vehicle (2% Ethanol)).
- Group 2: TA (1.0 mg/10 g diet (Ethanol vehicle)).
- Group 3: Rotenone (500 μ M).
- Group 4: TA (1.0 mg/10 g diet) + Rotenone (500 μ M).

(50 flies/replicate, n = 5).

Thereafter, the flies were anaesthetized in ice, weighed, homogenized in 0.1 M potassium phosphate buffer (pH 7.4, 1 mg:10 μ L buffer) and processed as described above for the determination of MTT assay and the following oxidative stress and antioxidant markers- H_2O_2 , NPSHs, T-SHs, protein carbonyls, malondialdehyde (MDA), NO (nitrate and nitrite), catalase and GST as well as AChE and emergence rate.

Measurement of longevity and survival rate of *D. melanogaster* after exposure to TA and rotenone. Both sexes of *D. melanogaster* (Harwich strain) 1- to 3-day old, were divided into different groups (50 flies/replicate, n = 5), and treated separately with ethanol (2.0%, control) and TA (0.1, 0.5, 1.0, 2.5, 10, and 20 mg/10 g diet) and rotenone (0, 250 and 500 μ M), respectively. The flies were changed at least once per week into diets containing similar concentrations of TA and rotenone. The flies were monitored and mortality was recorded daily, and used to plot the longevity curve for TA and 30 days survival rate for rotenone. The data were presented as a percentage of the control⁹.

Measurement of locomotor activity. Locomotor activity of TA- and rotenone-exposed flies was determined by employing the method of Feany and Bender²⁶. Briefly, ten flies from the control and treated groups were briefly immobilised using ice and separately placed in labelled glass column of 15 cm length and 1.5 cm in diameter. The flies were allowed to recover from anaesthesia and gently tapped to the bottom of the column. Thereafter, the number of flies that climbed up to the 6 cm mark and those below this mark were recorded. The data were then expressed as percentage of flies that crossed up to and beyond the 6 cm mark of the column.

Biochemical parameters. Total protein determination. Total protein was determined according to the methods of Lowry et al.⁵¹ using Bovine Serum Albumin as standard. The values of the total proteins for samples were used to calculate the activities of the antioxidant enzymes.

Determination of total thiols and non-protein thiol contents of *D. melanogaster* exposed to rotenone and TA. The levels of total and non-protein thiols were determined based on the method of Ellman⁵². The reaction mixture was made up of 170 μ L of 0.1 M potassium phosphate buffer (pH 7.4), 20 μ L of sample, and 10 μ L of DTNB. The reaction was allowed to incubate for 30 min at room temperature, and the absorbance was measured at 412 nm in a SpectraMax microplate reader (Molecular devices). To determine the non-protein thiol content, samples were precipitated with 4% sulphosalicylic acid (4%, ratio 1:1) and centrifuged for 10 min at 5000 rpm at 4 °C. The assay mixture for non-protein thiols consisted of 550 μ L of 0.1 M phosphate buffer, 100 μ L of supernatant and 100 μ L of DTNB. For both total and non-protein thiols, GSH was used as standard, and the data were expressed as in μ mol/mg of protein.

Determination of glutathione-S-transferase activity of *D. melanogaster* exposed to rotenone and TA. The GST activity was assessed according to Habig and Jakoby⁵³ with the use of 1-chloro-2,4-dinitrobenzene (CDNB) as substrate. The reaction mixture was contained 270 μ L of solution A (20 mL of 0.25 M potassium phosphate buffer, pH 7.0, with 2.5 mM EDTA, 10.5 mL of distilled water and 500 μ L of 0.1 M GSH at 25 °C), 20 μ L of the sample (1:5 dilution), and 10 μ L of 25 mM CDNB. The reaction was monitored at 340 nm for 5 min at 10 s intervals in a SpectraMax microplate reader (Molecular devices). The data were expressed as μ mol/min/mg protein.

Determination of catalase activity of *D. melanogaster* exposed to rotenone and TA. The activity of catalase was carried out using the method of Aebi⁵⁴. This was based on the clearance of hydrogen peroxide in the presence of catalase. The reaction mixture was made up of 1800 μ L of 50 mM phosphate buffer (pH 7.0), 180 μ L of 300 mM H_2O_2 , and 20 μ L of sample (1:50 dilution). The loss in absorbance of hydrogen peroxide was monitored at 240 nm, for 2 min at 10 s intervals and at 25 °C with a UV/Visible spectrophotometer. The catalase activity was expressed as μ mol of H_2O_2 consumed/min/mg protein.

Determination of hydrogen peroxide level of *D. melanogaster* exposed to rotenone and TA. The protocol by Wolff⁵⁵ was used to estimate H_2O_2 level. The reaction mixture contained 590 μ L of FOX-1 (Ferrous Oxidation-Xylenol orange) reagent and 10 μ L of sample. This was followed by 30 min incubation at room temperature, and the absorbance measured at 560 nm. The concentration of hydrogen peroxide generated was determined using extinction coefficient of H_2O_2 and expressed as μ mol/mL.

Determination of nitric oxide (nitrate/nitrite) level of *D. melanogaster* exposed to rotenone and TA. Nitric oxide (nitrate and nitrite) was quantified using Griess reaction following the protocol described at Green et al.⁵⁶. The fly homogenates were incubated in Griess reagent at room temperature for 20 min, and the absorbance measured at 550 nm. The concentration of NO in the samples were calculated using the standard calibration curve of $NaNO_2$ and expressed as μ mol/L.

Determination of acetylcholinesterase (AChE) activity of *D. melanogaster* exposed to rotenone and TA. AChE activity was determined with the method of Ellman et al.⁵⁷ The reaction contained 135 μ L of distilled water, 20 μ L of 100 mM potassium phosphate buffer (pH 7.4), 10 mM DTNB (20 μ L), 5 μ L of sample and 20 μ L of 8 mM acetylthiocholine as initiator. The reaction was monitored for 5 min at 15 s intervals at

412 nm using a SpectraMax microplate reader (Molecular devices). The enzyme activity was estimated as μmol of acetylthiocholine hydrolyzed/min/mg protein.

Determination of malondialdehyde level of *D. melanogaster* exposed to rotenone and TA. Lipid peroxidation was determined as previously discussed by Ohkawa et al.⁵⁸ by measuring the formation of Thiobarbituric Acid Reactive Substances (TBARS). The reaction mixture contained of 5 μL of 10 mM Butyl-hydroxytoluene (BHT), 200 μL of 0.67% thiobarbituric acid, 600 μL of 1% O-phosphoric acid, 105 μL of distilled water and 90 μL of supernatant. The mixture was incubated at 90 °C for 45 min and the absorbance was measured at 535 nm in a spectrophotometer. The data were expressed as μmol of MDA/L.

Determination of protein carbonyl content of *D. melanogaster* exposed to rotenone and TA. Estimation of Protein Carbonyl (PC) content was done following the method of Dalle-Donne et al.⁵⁹. The samples were added to trichloroacetic acid (20%) to precipitate the proteins. The reaction of the carbonyl group with 2, 4-dinitrophenylhydrazine to yield a stable dinitrophenylhydrazone. This was then mixed with guanidine hydrochloride (6 M) and the absorbance was measured at 375 nm. Protein Carbonyl content was quantified using the molar absorption coefficient of 22,000 $\text{M}^{-1} \text{cm}^{-1}$.

Determination of mitochondrial metabolic rate (cell viability) of *D. melanogaster* exposed to rotenone and TA. Mitochondrial metabolic rate (cell viability) was determined based on enzymatic reduction of MTT (3-(4,5-dimethylthiazol-2-yl)-2,5-diphenyltetrazolium bromide) to MTT-formazan in flies at a final concentration of 5 mg/mL according to Abe and Matsuki⁵⁸. The data were expressed as a percentage of the control.

Measurement of emergence rate of *D. melanogaster* exposed to rotenone and TA. The emergence rate of the progenies of flies into adulthood were also investigated after parent flies were treated with both TA and/or rotenone as previously reported⁴⁹. Briefly, 1 to 3 days old of 10 males and 10 female flies/ vial (5 replicates) were placed in diets containing similar doses of rotenone and TA as described above for 24 h. The flies were then removed from the diets while the embryos were allowed to develop to adulthood. The number of newly emerged flies from each vial were then recorded over a period of 2 weeks and expressed as percentage of control.

Molecular docking. Molecular docking analysis was performed to further investigate the anti-inflammatory capacity of TA by determining its binding affinity for some inflammatory protein targets (TNF- α , Caspase-1 and Cox-2) as compared to their respective standard inhibitors (Rofecoxib, Pralnacasan and Thalidomide). The grid box was set based on the protein structural dimensions and each ligand was set to have eight exhaustive conformations before being forwarded for docking using auto-dock vina in the PyRx workspace. The 3D structures of the protein–ligand complexes were prepared using the Chimera 1.14 workspace, and this was followed by visualization of the ligand–protein interactions and generation of the 2D structure using the Discovery Studio 2020.

Ligands and protein mining. The structure data file (SDF) format for the natural compound (TA) and inhibitors of TNF- α (Rofecoxib), Caspase-1 (Pralnacasan) and Cox-2 (Thalidomide) were downloaded from the PubChem database. The 3D crystal structures, also in SDF format, for TNF- α (PDB ID: 2AZ5), Caspase-1 (PDB ID: 1ICE) and Cox-2 (PDB ID: 5KIR) of humans (*Homo sapiens*) were obtained from the RCSB protein data bank (PDB), whereas the amino acid sequence of the protein homologues of the same protein targets for *D. melanogaster* were obtained from the UniProt webserver and their homology models were generated using the SWISS-MODEL webserver.

Ligand and protein preparation. Individual 3D structures of the selected protein targets were uploaded onto Chimera 1.14 workspace in order to prepare them for docking and they were converted into PDBQT format using the PyRx software. The ligands were also imported onto the PyRx workplace accordingly and converted to PDBQT format using the Open Babel plugin. Then, the proteins and ligands in PDBQT format were selected and forwarded for grid box generation.

Statistical analysis. Data were expressed as mean \pm standard deviation. One-way ANOVA (Analysis of Variance) followed by Tukey's post hoc test was utilized to calculate the significant differences among groups under various treatments. Statistically significant difference was set at $p < 0.05$, using the GraphPad Prism5.0 software.

Data availability

The datasets generated during and/or analysed during the current study are available from the corresponding author on reasonable request.

Received: 16 November 2021; Accepted: 7 March 2022

Published online: 17 March 2022

References

- Tanner, C. M. *et al.* Rotenone, paraquat, and Parkinson's disease. *Environ. Health Perspect.* **119**(6), 866–872. <https://doi.org/10.1289/ehp.1002839> (2011).
- Farwana, V. & Cannon, J. R. Rotenone neurotoxicity: Relevance to Parkinson's disease. *Adv. Neurotoxicol.* **4**, 209–254. <https://doi.org/10.1016/bs.ant.2019.11.004> (2020).
- Caboni, P. *et al.* Rotenone, deguelin, their metabolites, and the rat model of Parkinson's disease. *Chem. Res. Toxicol.* **17**, 1540–1548. <https://doi.org/10.1021/tx049867r> (2004).
- Farombi, E. O. *et al.* Neuroprotective role of kolaviron in striatal redo-inflammation associated with rotenone model of Parkinson's disease. *Neurotoxicology* **73**, 132–141. <https://doi.org/10.1016/j.neuro.2019.03.005> (2019).
- Ighodaro, O. M. & Akinloye, O. A. First line defence antioxidants-superoxide dismutase (SOD), catalase (CAT) and glutathione peroxidase (GPX): Their fundamental role in the entire antioxidant defence grid. *Alex. J. Med.* **54**, 287–293. <https://doi.org/10.1016/j.ajme.2017.09.001> (2018).
- Javed, H., Azimullah, S., Haque, M. E. & Ojha, S. K. Cannabinoid type 2 (CB2) receptors activation protects against oxidative stress and neuroinflammation associated dopaminergic neurodegeneration in rotenone model of Parkinson's disease. *Front. Neurosci.* **10**, 1–14. <https://doi.org/10.3389/fnins.2016.00321> (2016).
- Heinz, S. *et al.* Mechanistic investigations of the mitochondrial complex I inhibitor rotenone in the context of pharmacological and safety evaluation. *Sci. Rep.* **7**, 1–13. <https://doi.org/10.1038/srep45465> (2017).
- Ling, Z. *et al.* Rotenone potentiates dopamine neuron loss in animals exposed to lipopolysaccharide prenatally. *Exp. Neurol.* **190**(2), 373–383. <https://doi.org/10.1016/j.expneurol.2004.08.006> (2004).
- Abolaji, A. O., Adedara, A. O., Adie, M. A., Vicente-Crespo, M. & Farombi, E. O. Resveratrol prolongs lifespan and improves 1-methyl-4-phenyl-1, 2, 3, 6-tetrahydropyridine-induced oxidative damage and behavioural deficits in *Drosophila melanogaster*. *Biochem. Biophys. Res. Commun.* **503**, 1042–1048. <https://doi.org/10.1016/j.bbrc.2018.06.114> (2018).
- Maoka, T. Carotenoids as natural functional pigments. *J. Nat. Med.* **74**(1), 1–16. <https://doi.org/10.1007/s11418-019-01364-x> (2020).
- Fakhri, S., Yosifova Aneva, I., Farzaei, M. H. & Sobarzo-Sánchez, E. The neuroprotective effects of astaxanthin: Therapeutic targets and clinical perspective. *Molecules* **24**, 1–19. <https://doi.org/10.3390/molecules24142640> (2019).
- Ambati, R. R., Phang, S. M., Ravi, S. & Aswathanarayana, R. G. Astaxanthin: Sources, extraction, stability, biological activities and its commercial applications—A review. *Mar. Drugs* **12**, 128–152. <https://doi.org/10.3390/md12010128> (2014).
- Stachowiak, B. & Szulc, P. Astaxanthin for the food industry. *Molecules* **26**(9), 2666. <https://doi.org/10.3390/molecules26092666> (2021).
- Yang, C. *et al.* Anti-inflammatory effects of different astaxanthin isomers and the roles of lipid transporters in the cellular transport of astaxanthin isomers in CaCo-2 cell monolayers. *J. Agric. Food Chem.* **67**, 6222–6231. <https://doi.org/10.1021/acs.jafc.9b02102> (2019).
- Rodríguez-Sifuentes, L., Marszałek, J. E., Hernández-Carbajal, G. & Chuck-Hernández, C. Importance of downstream processing of natural Astaxanthin for pharmaceutical application. *Front. Chem. Eng.* **2**, 601483. <https://doi.org/10.3389/fceng.2020.601483> (2021).
- Kidd, P. Astaxanthin, cell membrane nutrient with diverse clinical benefits and anti-aging potential. *Altern. Med. Rev.* **16**, 355–364 (2011).
- Camera, E. *et al.* Astaxanthin, canthaxanthin and β -carotene differently affect UVA-induced oxidative damage and expression of oxidative stress-responsive enzymes. *Exp. Dermatol.* **18**, 222–231. <https://doi.org/10.1111/j.1600-0625.2008.00790.x> (2009).
- Nishigaki, I. *et al.* Cytoprotective role of astaxanthin against glycated protein/iron chelate-induced toxicity in human umbilical vein endothelial cells. *Phytother. Res.* **24**, 54–59. <https://doi.org/10.1002/ptr.2867> (2010).
- Shen, H. *et al.* Astaxanthin reduces ischemic brain injury in adult rats. *FASEB J.* **23**, 1958–1968. <https://doi.org/10.1096/fj.08-123281> (2009).
- Park, J. S., Chyun, J. H., Kim, Y. K., Line, L. L. & Chew, B. P. Astaxanthin decreased oxidative stress and inflammation and enhanced immune response in humans. *Nutr. Metab.* **7**, 1–10 (2010).
- Zhang, X. S. *et al.* Astaxanthin alleviates early brain injury following subarachnoid hemorrhage in rats: Possible involvement of Akt/bad signaling. *Mar. Drugs* **12**, 4291–4310. <https://doi.org/10.3390/md12084291> (2014).
- Aryal, B. & Lee, Y. Disease model organism for Parkinson disease: *D. melanogaster*. *BMB Rep.* **52**, 250–258. <https://doi.org/10.5483/BMBRep.2019.52.4.204> (2019).
- Lee, H. *et al.* DNA copy number evolution in *Drosophila* cell lines. *Genome Biol.* **15**, 1–20. <https://doi.org/10.1186/gb-2014-15-8-r70> (2014).
- Abolaji, A. O. *et al.* Involvement of oxidative stress in 4-vinylcyclohexene-induced toxicity in *Drosophila melanogaster*. *Free Radic. Biol. Med.* **71**, 99–108. <https://doi.org/10.1016/j.freeradbiomed.2014.03.014> (2014).
- Guo, M. What have we learned from *Drosophila* models of Parkinson's disease?. *Prog. Brain Res.* **184**, 2–16. [https://doi.org/10.1016/S0079-6123\(10\)84001-4](https://doi.org/10.1016/S0079-6123(10)84001-4) (2010).
- Feany, M. B. & Bender, W. W. A *Drosophila* model of Parkinson's disease. *Nature* **404**, 394–398. <https://doi.org/10.1038/35006074> (2000).
- Coulom, H. & Birman, S. Chronic exposure to rotenone models sporadic Parkinson's disease in *Drosophila melanogaster*. *J. Neurosci.* **24**, 10993–10998. <https://doi.org/10.1523/JNEUROSCI.2993-04.2004> (2004).
- Huangfu, J. *et al.* Antiaging effects of astaxanthin-rich alga *Haematococcus pluvialis* on fruit flies under oxidative stress. *J. Agric. Food Chem.* **61**, 7800–7804. <https://doi.org/10.1021/jf402224w> (2013).
- Sorrenti, V. *et al.* Astaxanthin as a putative geroprotector: Molecular basis and focus on brain aging. *Mar. Drugs* **18**(7), 351. <https://doi.org/10.3390/md18070351> (2020).
- Perez-Lloret, S. & Barrantes, F. J. Deficits in cholinergic neurotransmission and their clinical correlates in Parkinson's disease. *NPJ Parkinson's Dis.* **2**, 1–12. <https://doi.org/10.1038/nnpjparkd.2016.1> (2016).
- Rizzi, G. & Tan, K. R. Dopamine and acetylcholine, a circuit point of view in Parkinson's disease. *Front. Neural Circuits* **11**, 1–14. <https://doi.org/10.3389/fncir.2017.00110> (2017).
- Kumar, P. P. & Prashanth, K. H. Diet with low molecular weight chitosan exerts neuromodulation in rotenone-induced *Drosophila* model of Parkinson's disease. *Food Chem. Toxicol.* **146**, 1–8. <https://doi.org/10.1016/j.fct.2020.111860> (2020).
- Abolaji, A. O. *et al.* Protective role of resveratrol, a natural polyphenol, in sodium fluoride-induced toxicity in *Drosophila melanogaster*. *Exp. Biol. Med.* **244**, 1688–1694. <https://doi.org/10.1177/1535370219890334> (2019).
- Nagy, L., Nagata, M. & Szabo, S. Protein and non-protein sulfhydryls and disulfides in gastric mucosa and liver after gastrotoxic chemicals and sucralfate: Possible new targets of pharmacologic agents. *World J. Gastroenterol.* **13**, 1–8. <https://doi.org/10.3748/wjg.v13.i14.2053> (2007).
- Martin, H. L. & Teismann, P. Glutathione—A review on its role and significance in Parkinson's disease. *FASEB J.* **23**, 3263–3272. <https://doi.org/10.1096/fj.08-125443> (2009).
- Yang, Y. & Guan, X. Non-protein thiol imaging and quantification in live cells with a novel benzofurazan sulfide triphenylphosphonium fluorogenic compound. *Anal. Bioanal. Chem.* **409**, 3417–3427. <https://doi.org/10.1007/s00216-017-0285-y> (2017).

37. Johnson, W. M., Wilson-Delfosse, A. L. & Mieyal, J. Dysregulation of glutathione homeostasis in neurodegenerative diseases. *Nutrients* **4**, 1399–1440. <https://doi.org/10.3390/nu4101399> (2012).
38. Hosamani, R. Neuroprotective efficacy of *Bacopa monnieri* against rotenone induced oxidative stress and neurotoxicity in *Drosophila melanogaster*. *Neurotoxicology* **30**, 977–985. <https://doi.org/10.1016/j.neuro.2009.08.012> (2009).
39. Dalle-Donne, I., Rossi, R., Giustarini, D., Milzani, A. & Colombo, R. Protein carbonyl groups as biomarkers of oxidative stress. *Clin. Chim. Acta* **329**, 23–38. [https://doi.org/10.1016/s0009-8981\(03\)00003-2](https://doi.org/10.1016/s0009-8981(03)00003-2) (2003).
40. Levine, R. L. & Stadtman, E. R. Oxidative modification of proteins during aging. *Exp. Gerontol.* **36**, 1495–1502. [https://doi.org/10.1016/s0531-5565\(01\)00135-8](https://doi.org/10.1016/s0531-5565(01)00135-8) (2001).
41. Eleftherianos, I. *et al.* Nitric oxide levels regulate the immune response of *Drosophila melanogaster* reference laboratory strains to bacterial infections. *Infect. Immun.* **82**, 4169–4181. <https://doi.org/10.1128/IAI.02318-14> (2014).
42. Choi, B. M., Pae, H. O., Jang, S. I., Kim, Y. M. & Chung, H. T. Nitric oxide as a pro-apoptotic as well as anti-apoptotic modulator. *BMB Rep.* **35**, 116–126. <https://doi.org/10.5483/bmbrep.2002.35.1.116> (2002).
43. Natarajan, K., Abraham, P., Kota, R. & Isaac, B. NF- κ B-iNOS-COX2-TNF α inflammatory signaling pathway plays an important role in methotrexate induced small intestinal injury in rats. *Food Chem. Toxicol.* **118**, 766–783. <https://doi.org/10.1016/j.fct.2018.06.040> (2018).
44. Molla, M. D. *et al.* Role of caspase-1 in the pathogenesis of inflammatory-associated chronic noncommunicable diseases. *J. Inflamm. Res.* **13**, 1–16. <https://doi.org/10.2147/JIR.S277457> (2020).
45. Qiao, Y. C. *et al.* The change of serum tumor necrosis factor alpha in patients with type 1 diabetes mellitus: A systematic review and meta-analysis. *PLoS One* **12**, 1–14. <https://doi.org/10.1371/journal.pone.0176157> (2017).
46. Troncoso-Escudero, P., Parra, A., Nassif, M. & Vidal, R. L. Outside in: Unraveling the role of neuroinflammation in the progression of Parkinson's disease. *Front. Neurol.* **9**, 1–15. <https://doi.org/10.3389/fneur.2018.00860> (2018).
47. Sarbishegi, M. & Charkhat Gorgich, E. A. The effects of Celecoxib on rotenone-induced rat model of Parkinson's disease: Suppression of neuroinflammation and oxidative stress-mediated apoptosis. *Gene Cell Tissue Eng.* **6**, 1–6. <https://doi.org/10.5812/gct.92178> (2019).
48. Ardestani, M. S. Parkinson's disease, the inflammatory pathway and anti-inflammatory drug: An overview. *J. Med. Sci.* **10**, 49–58. <https://doi.org/10.3923/jms.2010.49.58> (2010).
49. Wang, W. *et al.* Caspase-1 causes truncation and aggregation of the Parkinson's disease-associated protein α -synuclein. *Proc. Natl. Acad. Sci.* **113**, 9587–9592. <https://doi.org/10.1073/pnas.1610099113> (2016).
50. Yunta, M. J. Docking and ligand binding affinity: Uses and pitfalls. *Am. J. Mode Optim.* **4**, 74–114. <https://doi.org/10.12691/ajmo-4-3-2> (2016).
51. Lowry, O. H., Rosebrough, N. J., Farr, A. L. & Randall, R. J. Protein measurement with the Folin phenol reagent. *J. Biol. Chem.* **193**, 265–275. [https://doi.org/10.1016/S0021-9258\(19\)52451-6](https://doi.org/10.1016/S0021-9258(19)52451-6) (1951).
52. Ellman, G. E. Tissue sulphhydryl groups. *Arch. Biochem. Biophys.* **82**, 70–77. [https://doi.org/10.1016/0003-9861\(59\)90090-6](https://doi.org/10.1016/0003-9861(59)90090-6) (1959).
53. Habig, W. H. & Jakoby, W. B. Assays for differentiation of glutathione S-transferases. *Methods Enzymol.* **77**, 398–405. [https://doi.org/10.1016/s0076-6879\(81\)77053-8](https://doi.org/10.1016/s0076-6879(81)77053-8) (1981).
54. Aebi, H. Catalase in vitro. *Methods Enzymol.* **105**, 121–126. [https://doi.org/10.1016/s0076-6879\(84\)05016-3](https://doi.org/10.1016/s0076-6879(84)05016-3) (1984).
55. Wolff, S. P. Ferrous ion oxidation in presence of ferric ion indicator xylenol orange for measurement of hydroperoxides. *Methods Enzymol.* **233**, 182–189. [https://doi.org/10.1016/S0076-6879\(94\)33021-2](https://doi.org/10.1016/S0076-6879(94)33021-2) (1994).
56. Green, L. C. *et al.* Analysis of nitrate, nitrite, and nitrate in biological fluids. *Anal. Biochem.* **126**, 131–138. [https://doi.org/10.1016/0003-2697\(82\)90118-x](https://doi.org/10.1016/0003-2697(82)90118-x) (1982).
57. Ellman, G. L., Courtney, K. D., Andres, V. Jr. & Featherstone, R. M. A new and rapid colorimetric determination of acetylcholinesterase activity. *Biochem. Pharmacol.* **7**, 88–95. [https://doi.org/10.1016/0006-2952\(61\)90145-9](https://doi.org/10.1016/0006-2952(61)90145-9) (1961).
58. Ohkawa, H., Ohishi, N. & Yagi, K. Assay for lipid peroxides in animal tissues by thiobarbituric acid reaction. *Anal. Biochem.* **95**(2), 351–358. [https://doi.org/10.1016/0003-2697\(79\)90738-3](https://doi.org/10.1016/0003-2697(79)90738-3) (1979).
59. Abe, K. & Matsuki, N. Measurement of cellular 3-(4, 5-dimethylthiazol-2-yl)-2, 5-diphenyl-tetrazolium bromide (MTT) reduction activity and lactate dehydrogenase release using MTT. *Neurosci. Res.* **38**, 325–329. [https://doi.org/10.1016/s0168-0102\(00\)00188-7](https://doi.org/10.1016/s0168-0102(00)00188-7) (2000).

Acknowledgements

This work was fully supported by the Cambridge Africa Alborada Research Fund, U.K. awarded to A.O.A. and A.J.W. A.J.W. is also supported by M.R.C. core funds (MC_UU_00015/6).

Author contributions

T.C.A., O.O.B. and A.A. performed experiments and analysed the data, with assistance from T.A.O., O.P.A. and A.T. Also, O.E.A. and T.O.J. carried out molecular docking analysis. In addition, A.O.A. and A.J.W. conceived the study, and designed experiments, while A.O.A. supervised the work. Moreover, O.O.B., T.C.A. and O.E.A. wrote the manuscript with input from all authors. T.C.A. and O.O.B. had Equal Contributions.

Competing interests

The authors declare no competing interests.

Additional information

Correspondence and requests for materials should be addressed to A.J.W. or A.O.A.

Reprints and permissions information is available at www.nature.com/reprints.

Publisher's note Springer Nature remains neutral with regard to jurisdictional claims in published maps and institutional affiliations.



Open Access This article is licensed under a Creative Commons Attribution 4.0 International License, which permits use, sharing, adaptation, distribution and reproduction in any medium or format, as long as you give appropriate credit to the original author(s) and the source, provide a link to the Creative Commons licence, and indicate if changes were made. The images or other third party material in this article are included in the article's Creative Commons licence, unless indicated otherwise in a credit line to the material. If material is not included in the article's Creative Commons licence and your intended use is not permitted by statutory regulation or exceeds the permitted use, you will need to obtain permission directly from the copyright holder. To view a copy of this licence, visit <http://creativecommons.org/licenses/by/4.0/>.

© The Author(s) 2022